RESEARCH ARTICLE

Carbonaceous aerosol composition over northern China in spring 2012

Yuhong Guo

Abstract The organic carbon (OC) and elemental carbon (EC) collected by eight-stage air samplers over northern China during spring 2012 were determined to characterize the spatial variations, size distributions, and sources of carbonaceous aerosols. OC and EC had high concentration levels and spatial heterogeneity. Higher carbonaceous aerosol loadings were found in urban areas, and high concentrations of OC and EC were found in eastern parts of northern China, including Beijing, Taiyuan in Shanxi Province, Yucheng in Shandong Province, Xianghe in Hebei Province, and Shenyang in Liaoning Province. Except the Cele site, OC and EC at all the sites showed a bimodal distribution, peaking in the size of 0.4–0.7 and 4.7–5.8 μm. Carbonaceous aerosols in the fine mode in the urban areas are mostly presented in smaller sizes than those in the rural/regional background areas. For most sites, mass median aerodynamic diameter (MMAD) values in the fine particles for OC were higher than those for EC with the addition of semi-volatile organics. Good correlations between OC and EC in all the cities (5 in North China and 1 in northeast China) may suggest the impact of anthropogenic emissions on carbonaceous aerosols in the above regions.

Y. Guo (✉)
State Key Laboratory of Atmospheric Boundary Layer Physics and Atmospheric Chemistry, Institute of Atmospheric Physics, Chinese Academy of Sciences, Beijing 100029, People's Republic of China
e-mail: tsguoyh@163.com

Introduction

Carbonaceous aerosol is among the major constituents of atmospheric particle (Saylor et al. 2006; Schwier et al. 2010). Particulate carbonaceous species have triggered more crucial environmental problems of particular concern, having a close connection with human health issues for its longer lifetime in the atmosphere and easy penetration into human lung (Künzi et al. 2013). Carbonaceous particles consist of a complex mixture of chemical compounds and are usually divided into two major fractions. Elemental carbon (EC) derives from the incomplete combustion of carboniferous materials, such as coal, gasoline, and diesel, and the burning of biomass. Particulate organic carbon (OC) can be emitted from primary sources, especially incomplete combustion of fossil fuels, or formed in the oxidation process of volatile organic compounds followed by condensing on preexisting aerosol (Jiang et al. 2012; Kroll and Seinfeld 2008).

Carbonaceous aerosol is not only a pollutant but also an important driver of global change. It has long been known that EC is referred to as absorbing component while OC is associated with optical scattering until absorbing organic components have been recognized (Andreae and Gelencsér 2006; Sun et al. 2007; Yang et al. 2009). Absorption of solar radiation by carbonaceous aerosols may heat the atmosphere, thereby altering the vertical temperature profile, while scattering of solar radiation may lead to a net cooling of the atmosphere/ocean system. Besides directly by scattering or absorbing light, carbonaceous particles also affect the Earth's radiative balance indirectly by acting as cloud condensation nuclei (CCN), thereby influencing the albedo and lifetime of clouds. Moreover, the influence of carbonaceous particles exerted on climate was also complicated by their changing mixing status

(Huang and Yu 2008; Leaitch et al. 2010; Yu et al. 2010). The evaluation of the health and climate impacts of carbonaceous aerosols is burdened with relatively large uncertainties due to very limited understanding of the regional and global distributions of carbonaceous aerosol.

In China, rapid economic growth and urbanization have been changing the physical, chemical, and optical characteristics of atmospheric environment (Wang et al. 2011a, b). Moreover, deserts over northern China are major emission sources of Asian dust. Thus, the aerosols over northern China in spring comprise complex compositions including anthropogenic and natural particles in a highly mixed condition. Estimates of health and climate effects of EC and OC in China are more uncertain in such a huge territory and high density population country, which makes quantifying the weather-climate effects of carbonaceous aerosol more difficult. The crux of understanding the distribution and climate effect of carbonaceous aerosol in China is the lack of a consistent measurement network in China with good spatiotemporal coverage like the Interagency Monitoring of Protected Visual Environments (IMPROVE) network in USA and EMEP in Europe. Carbonaceous aerosols in China have been studied at an increasing number of locations; however, these studies were mainly based on bulk $PM_{2.5}$ or PM_{10} and focus on the rapid economic growth and high population density (Li and Bai 2009; Zhou et al. 2012). So far, only two papers reported carbonaceous aerosols simultaneously at multiple locations across China in winter and summer and over an entire year, respectively (Cao et al. 2007; Zhang et al. 2008). They both concluded that high levels of OC and EC, and higher OC/EC ratios in China. To our best knowledge, there is no systematic atmosphere watch network which covers different ecosystems and provides size distribution information of carbonaceous particle in China although the wealth of measurements should be compiled to present us aerosol formation, growth, and removal which determine its health and climate effects. In the present study, OC and EC data collected in a spring season over northern China have been analyzed. The purpose of these measurements was to provide more useful data to reduce the uncertainties in quantification of carbonaceous aerosol health effect in northern China during spring.

Materials and methods

Site descriptions and aerosol sampling

The aerosol sampling was conducted across northern China from March to May, 2012. The locations of the observation network shown in Fig. 1 are summarized in details in Table 1. Size-segregated particles were collected at the sites using eight-stage air samplers (Andersen, USA) at an airflow rate of 28.3 L/min for 48 h from 9:00 a.m. Monday to 9:00 a.m. Wednesday bi-weekly, with cutoff points as 0.4, 0.7, 1.1, 2.1, 3.3, 4.7, 5.8, and 9.0 μm. The filtration media were 81-mm quartz microfiber filters (Munktell Filter AB, Swedish) which were cleaned by heating at 800 °C for 3 h before using.

Elemental carbon and organic carbon measurements

A thermal/optical carbon aerosol analyzer (DRI Model 2001A, Desert Research Institute, USA) was used to analyze EC and OC content. The temperature program for the thermal analysis followed the Interagency Monitoring of Protected Visual Environments (IMPROVE_A) protocol (Chow et al. 2004, 2007). A punch aliquot (0.50 cm^2) of a quartz fiber filter sample was heated stepwise in an oven at 140 °C (OC1), 280 °C (OC2), 480 °C (OC3), and 580 °C (OC4) in a pure helium atmosphere for OC volatilization and 580 °C (EC1), 740 °C (EC2), and 840 °C (EC3) in a 2 % oxygen-contained helium atmosphere for EC oxidation. At each stage, the CO_2 formed was catalytically converted to CH_4 by a MnO_2 catalyst, and the resulting CH_4 was then measured using a flame ionization detector (FID). The analyzer was calibrated using a standard mixture of CH_4 and CO_2 before and after sample analysis. The charring OC is little in my samples, so charring correction by optical correction was not made in this study. Field blank filters were also analyzed, and the sample results
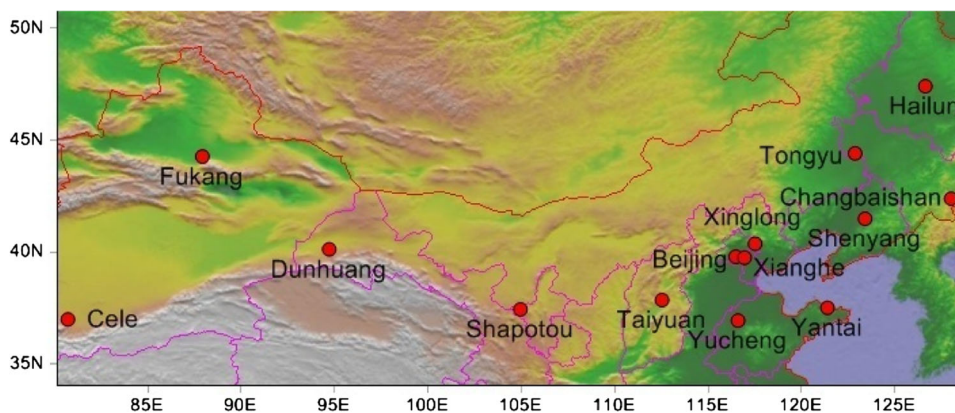

Fig. 1 Locations of sites over northern China

Table 1 Site and sampling descriptions

Station name	No. of sets	Coordinate	Region	Classification	Station description
Beijing (BJZ)	8	39.97° N, 116.37° E	North China	Urban	44 m asl, in Haidian District, Beijing, China
Xianghe (XHZ)	6	39.76° N, 116.95° E	North China	Rural	9 m asl, in Xianghe county of Hebei Province, China
Yantai (YTZ)	7	37.52° N, 121.39° E	North China	Urban	48 m asl, in Yantai City of Shandong Province, China
Taiyuan (TYZ)	6	37.87° N, 112.53° E	North China	Urban	800 m asl, in Taiyuan City of Shanxi Province, China
Yucheng (YCZ)	7	36.95° N, 116.6° E	North China	Rural	23 m asl, in Yucheng City of Shandong Province, China
Xinglong (XLZ)	9	40.38° N, 117.51° E	North China	Remote	879 m asl, in Xinglong county of Hebei Province, China
Shenyang (SHY)	6	41.5° N, 123.4° E	Northeastern China	Urban	41 m asl, in Shenyang City of Liaoning Province, China
Hailun (HLZ)	6	47.43° N, 126.63° E	Northeastern China	Rural	236 m asl, in Hailun City of Heilongjiang Province, China
Tongyu (TYU)	5	44.42° N, 122.87° E	Northeastern China	Remote	160 m asl, in Tongyu county of Jilin Province, China
Changbai Mountain (CBS)	4	42.4° N, 128.01° E	Northeastern China	Remote	738 m asl, near the Changbai Mountain Natural Reserve, Jilin Province, PR China
Dunhuang (DHZ)	7	40.13° N, 94.71° E	Northwestern China	Rural	1139 m asl, in Dunhuang City of Gansu Province, China; located in a hyperarid area at Kumtag Desert
Fukang (FKZ)	7	44.28° N, 87.92° E	Northwestern China	Rural	461 m asl, in Fukang City of Xinjiang, China; located in Gurbantünggüt desert
Shapotou (SPT)	6	37.45° N, 104.95° E	Northwestern China	Remote	1320 m asl, in Zhongwei County of Ningxia, China; located insouthern margin of Tengger desert
Cele (CLZ)	5	37° N, 80.72° E	Northwestern China	Remote	1302 m asl, in Cele County of Xinjiang, China; located in southern margin of Taklimakan Desert

were subtracted by the average blank concentrations, which were 1.8 ± 0.4 and 0.1 ± 0.1 µg m^{-3} for OC and EC, respectively.

Results and discussion

Spatial variations of concentration of OC and EC

Among all the sites, Taiyuan had the highest OC and EC concentrations, which is predominantly attributable to heavy coal consumption of industrial complexes from the power plants and chemical industrial plants (Meng et al. 2007). OC and EC in PM$_{9.0}$ in Taiyuan were 46.6 ± 5.3 and 11.6 ± 3.9, respectively. Xianghe is a distant suburb near Beijing City, and OC and EC at this station were higher than those in Beijing. Xianghe is heavily polluted due to both local and distant sources of fossil fuel combustion, vehicular and industrial emissions, and occasional dust and biomass fires (Yang et al. 2009). High average OC and EC were also found at the agricultural site (Yucheng, Shandong). This site stands for rural areas in China which has high income levels of peasants and rural population densities. Open biomass burning such as agricultural residues in Shandong Province may contribute to the high levels of EC and OC at this agricultural site (Cao et al. 2006). Agricultural field burning appeared in part of Shandong and Hebei Provinces could exert influence even on Beijing (Duan et al. 2004). In fact, biomass burning is ubiquitous in rural areas in China. As Zhang et al. (2012) reported, biomass

burning and anthropogenic emissions exerted influence on carbonaceous aerosols in desert area in northeastern China.

Very high OC and EC concentration levels were found in the North China Plain and Northeast China Plain. Many large cities located in these regions, such as Beijing, Taiyuan, and Shenyang, had high OC and EC concentrations. Some rural areas in the above plains also had high OC and EC concentrations, such as Yucheng and Xianghe. This matched with the BC emission inventory very much, in which very high emission densities can be found in the North China Plain, Northeast Plain, and Shanxi Highland (Wang et al. 2012). Also, relatively high BC emissions can be found in almost all large cities and populated rural areas, such as those in the Provinces of Shandong, and Shanxi, where rural solid fuel burning and coke ovens are the major sources (Wang et al. 2012).

Sites in Northwest China (including Dunhuang, Fukang, Shapotou, and Cele) had lower OC and EC concentration levels than those in North China and northeastern China. However, compared to other sites in desert regions around the world, the EC and OC concentrations were higher in this study. For instance, EC and OM in PM$_{2.5}$ in Nagarkot during spring were 1.5 and 23 µg/m^3, respectively (Carrico et al. 2003). PM$_{2.5}$ EC and OC in a desert region in northern Chile between December 17, 2007 and January 20, 2008 were 1.084 and 3.728 µg/m^3, respectively (Jorquera and Barraza 2013). In Israel and Jordan, the annual average results in PM$_{2.5}$ were as follows: Eilat, 0.82 µg EC/m^3 and 3.3 µg OC/m^3; Aqabah, 0.92 µg EC/m^3 and 3.7 µg OC/m^3; and Rachma, 0.45 µg EC/m^3 and 2.2 µg OC/m^3 (Schneidemesser et al. 2010).

According to the EC tracer method, primary organic carbon (POC) and secondary organic carbon (SOC) were calculated (Table 2) (Turpin et al. 1991; Cabada et al. 2004). The averaged fractions of SOC showed that the contributions from SOC to OC loadings were in the range of 30.7 % (in Xianghe) and 80.9 % (in Fukang). Although SOC estimation is burdened with substantial uncertainty using EC tracer method, it still suggested an important role of secondary organic aerosol (SOA) formation in China, especially in rural areas. In the urban regions, such as Shenyang and Taiyuan, POC had high percentages (32.1±17.1 and 39.2±21.3 %, respectively), indicating high OC and EC emissions. In Xianghe, SOC accounted for 30.7±13.3 % of OC. This figure was lower than those of urban sites and may reflect local anthropogenic emissions in rural area.

Size distributions of OC and EC

Size distributions of EC and OC could reflect the emission sources, formation, and growth mechanism of aerosol particles. Also, the information of OC and EC may be helpful in understanding the role particulate carbon plays in urban, regional, and global climate change.

Due to absence of cutoff size of 2.5 μm in Andersen eight-stage air samplers, fine and coarse particles are defined as particles with sizes <2.1 and >2.1 μm, respectively. Figure 2 presents size distributions of OC and EC at all the sites during spring periods. Except for the Cele site, EC at all the sites showed a bimodal distribution with primary mode in the size range of 0.4–1.1 μm and secondary mode in the size of 4.7–5.8 μm and stood for fine and coarse modes, respectively.

Table 2 Averaged daily concentrations (μg/m^3) for EC, POC, and SOC in PM$_9$ in the spring

	EC	POC	SOC	SOC/OC (%)
Beijing	5.8±3.9	23.8±14.7	14.7±6.8	41.7±17.0
Yantai	6.3±2.4	13.1±5.4	12.6±8.5	46.0±22.3
Taiyuan	11.6±3.9	28.9±8.9	19.5±11.2	39.2±21.3
Xianghe	6.9±2.8	33.5±8.1	14.5±6.0	30.7±13.3
Yucheng	9.2±2.0	8.5±1.9	17.1±12.8	56.9±24.2
Xinglong	3.3±2.3	4.1±1.0	7.5±2.4	63.9±10.1
Shenyang	9.6±2.2	26.1±5.9	15.0±11.3	32.1±17.1
Hailun	6.9±2.3	4.5±1.3	5.2±1.9	52.6±10.7
Tongyu	3.8±1.2	11.4±3.1	11.4±7.4	44.7±29.1
Changbai Mountain.	2.6±0.9	3.3±2.1	4.2±1.4	61.4±20.6
Dunhuang	6.2±3.0	10.7±5.7	11.1±4.3	51.8±17.9
Fukang	5.2±2.6	1.1±0.7	5.4±3.9	80.9±7.8
Shapotou	4.4±1.4	8.1±2.2	6.4±3.4	42.0±18.4
Cele	2.8±0.7	6.6±2.2	8.6±9.7	47.6±16.3

EC elemental carbon, *POC* primary organic carbon, *SOC* secondary organic carbon, *OC* organic carbon

The primary peak in fine mode EC predominantly indicated combustion processes, such as vehicular exhaust, coal combustion, and biomass burning. As mentioned above, fossil source may be relatively more important for urban areas and while biomass burning may have great influence on OC and EC in rural areas (Chen et al. 2013). Another peak in the coarse modes existed in the size range of 4.7–5.8 μm, albeit with a low mass fraction. Since the RH was below 40 %, the peak was not attributable to hygroscopic reaction which leads to growth in particle sizes. So the peak could have been caused by four reasons: (1) During impactor sampling, coarse EC as reaction interface, where many constituents are processed though heterogeneous reaction, produced all kinds of secondary products, such as SOC, sulfate, and natrate. Thus, internal mixture absorbed much more EC; (2) during impactor sampling, EC in fine modes was in adherence to coarse modes; (3) re-suspension of EC-containing soil/dust particles and tire abrasion in road dusts (Glaser et al. 2005). Han et al. (2009) reported that road dust corresponded well with the human emission sources, showing high EC levels; (4) in China, lower combustion efficiency is another reason for coarse soot.

Except for Cele, OC at all the sites also showed a bimodal distribution with primary mode in the size range of 0.4–1.1 μm and secondary mode in the size of 4.7–5.8 μm, respectively. OC showed a large peak in many sites, such as Beijing, Shenyang, and Xianghe. This may indicate the effect of dust on the size distribution of OC. Yan et al. (2012) found a similar phenomenon in Beijing during spring 2004.

OC and EC were concentrated in fine mode. Furthermore, EC was more enriched in fine mode. For instance, At the Yantai, Yucheng, and Xinglong sites, where the fine peaks were higher than the coarse ones, PM$_{2.1}$ EC accounted for 77 %, 73 %, and 71 % of PM$_{9.0}$ EC, respectively. The percentages for OC were 58 %, 59 %, and 64 %, respectively. This probably reflects the generally greater proportional contribution of coarse particles to PM mass at the urban sites due to particle re-suspension, industrial activity, etc. Furthermore, The percentages of OC and EC concentrated in fine mode were higher in Northwest China than in North China and northeastern China. This phenomenon may reflect the effect of dust on carbonaceous aerosols. Situated in a desert with considerable sources of dust around, it does not seem surprising that there would be significant coarse mode contributions at times. Spring is well known as an enhanced period of dust storms in that area of the world, and those storms can have very long range impacts. Therefore, there is a possibility that OC deposited on the desert dust may contribute to the results as well as the possibilities that OC is attached during dust transport or SOA is formed by reaction of VOCs on dust particles.
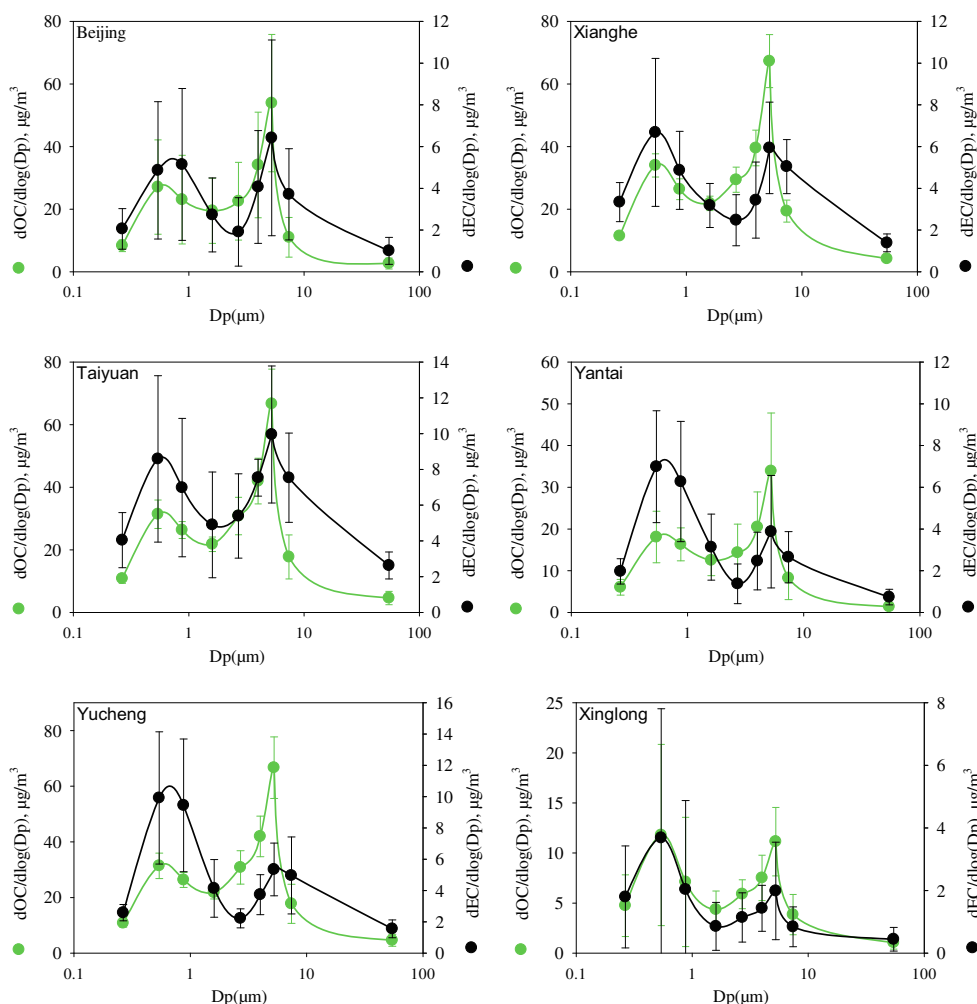
Fig. 2 Particle size distributions (dM/dlogDp) of OC and EC at all the observation sites

The mass median aerodynamic diameter (MMAD) values of OC and EC in the fine and coarse mode and total particle size range are presented in Table 3. The MMAD values of OC and EC in the fine mode ranges from 0.65 to 0.85 μm and from 0.51 to 0.85 μm, respectively. These size ranges were larger than typically emitted by primary sources, such as diesel, gasoline-powered cars, coal combustion, and biomass burning, which existed in the range of 0.1–0.52 μm (Hays et al. 2004; Hildemann et al. 1991; Kleeman et al. 2000; McElroy et al. 1982). This phenomenon indicated aged carbonaceous aerosols in this study.

Among all the sampling sites, MMAD values of EC and OC in the fine mode were smaller in the urban air and higher in the rural/remote sites. This may be due to the differences in their sources and atmospheric processes such as in-cloud processing during long-range atmospheric transport. In densely populated rural area in northern-central China where coal is in abundant supply, small domestic stoves are used for cooking and heating. Usually, coal combustion from these stoves has insufficient efficiencies and introduces larger EC particles. Another explanation is that when aerosol

particles containing EC are transported from high concentration urban areas to the rural sites, EC gets aged with extra OC or other ion coatings.

Relationship between OC and EC and OC/EC ratios

EC is directly emitted from combustion emission sources, so it has often been used as an indicator of POC. Therefore, relationship between OC and EC and OC/EC ratios can be used to indicate the emission sources of carbonaceous aerosol. Higher R^2 means stronger similarity of the emission sources of OC and EC.

Urban areas in China showed stronger correlations than rural/remote sites; for instance, strong correlations between OC and EC in PM$_{2.5}$ were observed in spring ($R^2=0.67$) and winter ($R^2=0.84$) in Shanghai (Hou et al. 2011). The correlation between OC and EC in PM$_{2.5}$ was significant ($R^2=0.90$ and 0.66 in autumn and winter, respectively) in Xi'an (Cao et al. 2005). These stronger correlations can be probably explained by similar dominant emissions from traffic and industry sources in urban and surrounding rural areas in the three
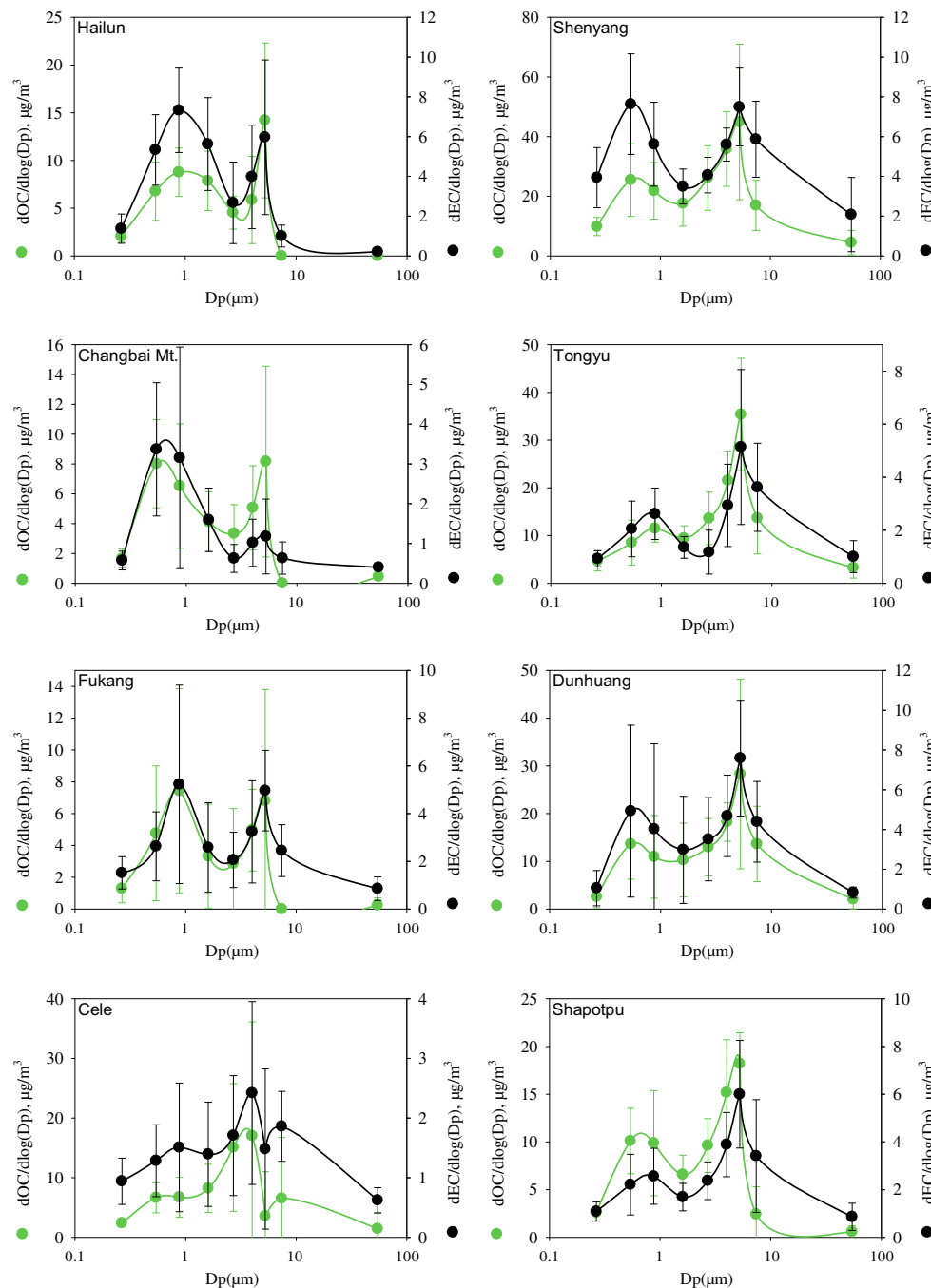
Fig. 2 (continued)

regions. Contrarily, the correlation between OC and EC in PM$_{2.5}$ in Daihai (a rural site) was moderate (R^2=0.41 in spring) (Han et al. 2008).

Correlations between OC and EC in northern China are depicted in Fig. 3 to examine the similarity between the OC and EC emission sources. Level of significance for the r^2 values was 0.05 for all the sites.

When the full data set of North China was separated into several data populations by particle sizes, the correlation coefficients would rise slightly. Despite the different locations of

the six monitoring stations, results in this study showed that the correlations between OC and EC were very similar among the urban sites. This similarity may be explained by the fact that this region is highly urbanized and this area is with strong influences of similar pollutant sources.

OC/EC ratio from biomass fire is 8.0 in spring according to the inventory of black carbon and organic carbon emissions from China (Cao et al. 2008). The average OC/EC ratios were 12.0 for long-range transport, 2.7 for coal combustion, and 1.1 for motor vehicles (Saarikoski et al. 2008;

Table 3 Mass median aerodynamic diameter (MMAD) values of EC and OC (μm)

	OC			EC		
	Total	Fine	Coarse	Total	Fine	Coarse
Beijing	1.89±0.37	0.66±0.13	4.28±1.15	1.83±1.13	0.62±0.15	6.49±1.22
Yantai	1.69±0.41	0.70±0.03	4.72±0.16	1.01±0.22	0.67±0.08	6.59±0.97
Taiyuan	2.23±0.52	0.68±0.05	4.83±0.19	2.73±1.45	0.55±0.08	6.85±0.86
Xianghe	2.26±0.41	0.65±0.05	4.88±0.08	1.59±0.85	0.58±0.21	6.90±1.38
Yucheng	1.85±0.34	0.76±0.12	4.88±0.35	1.20±0.44	0.69±0.12	7.39±0.59
Xinglong	1.49±0.70	0.71±0.17	4.93±0.54	1.94±2.07	0.71±0.68	6.19±2.15
Shenyang	2.29±0.48	0.65±0.04	5.08±0.90	1.60±0.58	0.51±0.05	6.92±2.45
Hailun	1.28±0.4	0.85±0.14	4.49±0.22	1.19±0.33	0.85±0.10	4.56±0.56
Tongyu	3.24±0.81	0.73±0.15	5.26±0.47	3.62±1.64	0.71±0.13	7.09±0.81
Changbai Mountain	1.09±0.26	0.68±0.09	4.40±0.23	1.12±0.42	0.71±0.12	7.60±1.29
Dunhuang	2.23±0.86	0.74±0.17	5.19±0.81	3.13±1.96	0.65±0.18	5.63±0.90
Fukang	1.45±1.18	0.70±0.17	4.04±0.76	2.19±1.38	0.69±0.14	6.26±1.36
Shapotou	1.92±0.60	0.73±0.06	4.16±0.30	3.20±1.19	0.66±0.14	5.82±0.92
Cele	2.05±1.15	0.80±0.12	3.23±1.72	2.31±0.80	0.71±0.38	8.30±5.55

EC elemental carbon, *OC* organic carbon

Watson et al. 2001) in field experimental measurements. Therefore, OC/EC ratios from coal combustion and motor were much lower than those from biomass burning and long-range transport which accompany decreasing EC and OC loading (Zhang et al. 2008).

The scatter plot between OC and EC concentrations in fine particle showed better correlation than in the coarse mode in northern China, especially at sites in North China, Shenyang, Dunhuang, and Fukang sites, implying common source contributions to EC and OC in fine mode due to anthropogenic activities. The weak correlation in northwestern China indicated that carbonaceous aerosols in this region have more varying source contributions. In North China, where population, vehicles, and industries are concentrated, coal combustion and motor may be the main source of carbonaceous aerosol. In Northeast and Northwest China populated rural areas, biomass burning may play a dominant role.

The OC/EC ratios in $PM_{1.1}$, $PM_{2.1}$, and $PM_{9.0}$ in this study were similar with those reported in the rural sites, but higher than those measured at the urban sites (Zhang et al. 2008). One reasonable explanation is that these sites were influenced by open biomass burning near them in spring. For instance, biomass burning is a significant repetitive pollution factor in Beijing (Duan et al. 2004). It is interesting that the OC/EC ratios in the fine particles were lower than those in the coarse particles with the aerodynamic diameter between 2.1 and 5.8 μm. A higher and increasing OC/EC ratio usually accompanies decreasing EC loading in the coarse particles. One explanation is that during long-range transport, the EC and OC concentrations are diluted with cleaner air. With the addition of semivolatile organics (primary or secondary) onto the preexisting

particles, the aged aerosol particles contain more OC, resulting in an increased OC/EC ratio in the coarse particles. OC/EC ratios at the Xinglong site were lower than those of Changbai Mountain and Cele for $PM_{1.1}$, $PM_{2.1}$, and $PM_{2.1-9.0}$, respectively. For instance, in submicron, OC/EC ratio was 3.9 at the Xinglong site, and the OC/EC ratios were 5.1 and 6.7 at the Changban Mountain and Cele sites, respectively. This may due to urbanization and industrialization in North China. In $PM_{2.1-9.0}$, OC/EC ratios at the Changbai Mountain and Cele sites were much higher than that of Xinglong. This may give some indication of biomass burning in the remote regions.

The relative amounts of optically absorbing carbon and optically scattering carbon control the direct radiative climate forcing effect of carbonaceous aerosol. Besides EC, a part of organic carbon (OC) strongly absorbs in the UV and visible wavelengths but has weak absorption in the near-infrared (IR) (Andreae and Gelencsér 2006; Sun et al. 2007; Yang et al. 2009). So caution needs to be exerted when assessing the impacts of carbonaceous aerosols in northern China on regional and global climate.

Conclusions

This study analyzed the spatial variations, size distributions, and characteristics of sources of carbonaceous aerosols on the basis of data over northern China during spring 2012. Both urban and rural areas of China showed higher concentrations of carbonaceous aerosols than clear sites in the world. A notable contrast between the urban and rural/regional background areas showed anthropogenic carbonaceous particle
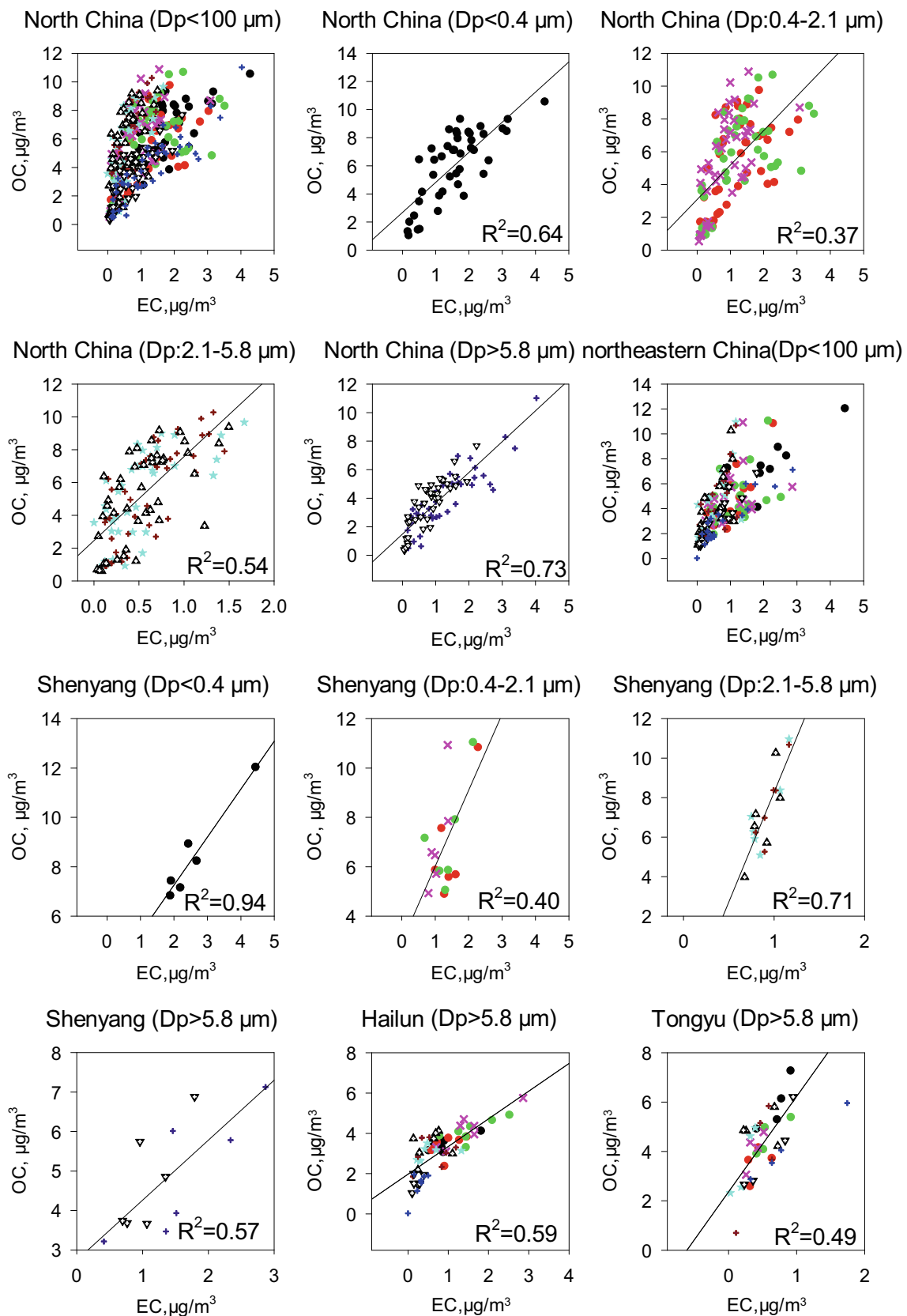
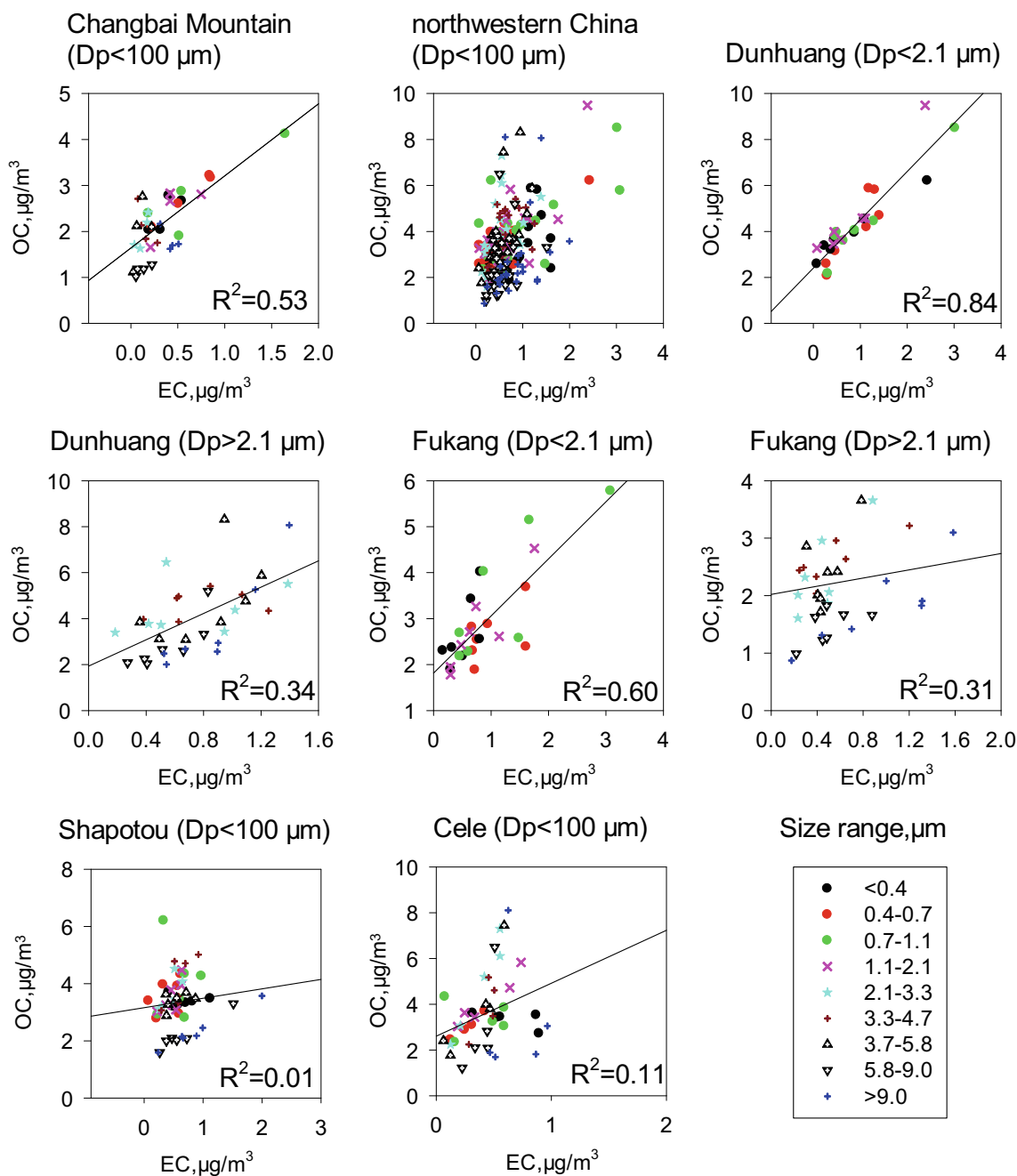Fig. 3 Correlations between EC and OC at the sites over northern China

Fig. 3 (continued)

pollutants in the densely populated and urbanized area. Among all the sites except Cele, OC and EC presented a bimodal distribution with two peaks at the sizes of 0.4–1.1 and >4.7 μm. OC and EC were mainly enriched in fine modes. Based on the calculation of the MMAD values for OC and EC, carbonaceous aerosols in the fine mode in the urban areas are mostly presented in smaller sizes than those in the rural// regional background areas. Such spatial variations demonstrated the differences in the sources and the atmospheric processes of OC and EC in different areas. Good correlations between OC and EC in all the cities (5 in North China and 1 in northeast China) may suggest the impact anthropogenic emissions on carbonaceous aerosols in the above regions. In the fine mode, lower OC/EC ratios and stronger correlations between OC and EC mainly arise from anthropogenic emissions, especially motor exhaust and coal combustion. In coarse mode, poor correlations between OC and EC and higher OC/EC ratios may indicate biomass burning and aerosol aging during spring. In North China, where population, vehicles, and industries are concentrated, coal combustion

and motor may be the main source of carbonaceous aerosol. In Northeast and Northwest China populated rural areas, biomass burning may play a dominant role.

References

Andreae MO, Gelencsér A (2006) Black carbon or brown carbon? The nature of light-absorbing carbonaceous aerosols. Atmos Chem Phys Discuss 6:3419–3463

Cabada JC, Pandis SN, Subramanian R, Robinson AL, Polidori A et al (2004) Estimating the secondary organic aerosol contribution to PM2. 5 using the EC tracer method special issue of aerosol science and technology on findings from the fine particulate matter supersites program. Aerosol Sci Technol 38(S1):140–155

Cao JJ, Chow JC, Lee S, Li Y, Chen SW, An ZS et al (2005) Characterization and source apportionment of atmospheric organic and elemental carbon during fall and winter of 2003 in Xi'an, China. Atmos Chem Phys Discuss 5:3561–3593

Cao GL, Zhang XY, Zheng FC (2006) Inventory of black carbon and organic carbon emissions from China. Atmos Environ 40:6516–6527

Cao JJ, Lee S, Chow JC, Watson JG, Ho KF, Zhang RJ et al (2007) Spatial and seasonal distributions of carbonaceous aerosols over China. J Geophys Res 112:D22S11

Cao GL, Zhang XY, Wang YQ, Zheng FC (2008) Estimation of emissions from field burning of crop straw in China. Chin Sci Bull 53: 784–790

Carrico CM, Bergin MH, Shrestha AB, Dibb JE, Gomes L, Harris JM (2003) The importance of carbon and mineral dust to seasonal aerosol properties in the Nepal Himalaya. Atmos Environ 37:2811–2824

Chen B, Andersson A, Lee M, Kirillova EN, Xiao Q, Kruså M, Shi M, Hu K, Lu Z, Streets DG (2013) Source forensics of black carbon aerosols from China. Environ Sci Technol 47(16):9102–9108

Chow JC, Watson JG, Chen L-WA, Arnott WP, Moosmüller H, Fung K (2004) Equivalence of elemental carbon by thermal/optical reflectance and transmittance with different temperature protocols. Environ Sci Technol 38(16):4414–4422

Chow JC, Watson JG, Chen L-WA, Chang MO, Robinson NF, Trimble D et al (2007) The IMPROVE_A temperature protocol for thermal/optical carbon analysis: maintaining consistency with a long-term database. Air Waste Manage Assoc 57(9):1014–1023

Duan FK, Liu XD, Yu T, Cachier H (2004) Identification and estimate of biomass burning contribution to the urban aerosol organic carbon concentrations in Beijing. Atmos Environ 38:1275–1282

Glaser B, Dreyer A, Bock M, Fiedler S, Mehring M, Heitmann T (2005) Source apportionment of organic pollutants of a highway-traffic-influenced urban area in Bayreuth (Germany) using biomarker and stable carbon isotope signatures. Environ Sci Technol 39(11):3911–3917

Han YM, Han ZW, Cao JJ, Chow JC, Watson JG, An ZS, Liu SX, Zhang RJ (2008) Distribution and origin of carbonaceous aerosol over a rural high-mountain lake area, Northern China and its transport significance. Atmos Environ 42(10):2405–2414

Han YM, Cao JJ, Chow JC, Watson JG, An ZS, Liu SX (2009) Elemental carbon in urban soils and road dusts in Xi'an, China and its implication for air pollution. Atmos Environ 43:2464–2470

Hays MD, Smith ND, Dong YJ (2004) Nature of unresolved complex mixture in size-distributed emissions from residential wood combustion as measured by thermal desorption-gas chromatography-mass spectrometry. J Geophys Res: Atmos 109:D16

Hildemann LM, Markowski GR, Jones MC, Cass GR (1991) Submicrometer aerosol mass distributions of emissions from boilers, fireplaces, automobiles, diesel trucks, and meat-cooking operations. Aerosol Sci Technol 14:138–152

Hou B, Zhuang GS, Zhang R, Liu TN, Guo ZG, Chen YJ (2011) The implication of carbonaceous aerosol to the formation of haze: revealed from the characteristics and sources of OC/EC over a mega-city in China. J Hazard Mater 190:529–536

Huang XF, Yu JZ (2008) Size distributions of elemental carbon in the atmosphere of a coastal urban area in South China: characteristics, evolution processes, and implications for the mixing state. Atmos Chem Phys 8:5843–5853

Jiang F, Liu Q, Huang XX, Wang TJ, Zhuang BL, Xie M (2012) Regional modeling of secondary organic aerosol over China using WRF/Chem. J Aerosol Sci 43:57–73

Jorquera H, Barraza F (2013) Source apportionment of PM$_{10}$ and PM$_{2.5}$ in a desert region in northern Chile. Sci Total Environ 444:327–335

Kleeman MJ, Schauer JJ, Cass GR (2000) Size and composition distribution of fine particulate matter emitted from motor vehicles. Environ Sci Technol 34:1132–1142

Kroll JH, Seinfeld JH (2008) Chemistry of secondary organic aerosol: formation and evolution of low-volatility organics in the atmosphere. Atmos Environ 42:3593–3624

Künzi L, Mertes P, Schneider S, Jeannet N, Menzi C, Dommen J et al (2013) Responses of lung cells to realistic exposure of primary and aged carbonaceous aerosols. Atmos Environ 68:143–150

Leaitch WR, Lohmann U, Russell LM, Garrett T, Shantz NC, Toom-Sauntry D et al (2010) Cloud albedo increase from carbonaceous aerosol. Atmos Chem Phys 10:7669–7684

Li WF, Bai ZP (2009) Characteristics of organic and elemental carbon in atmospheric fine particles in Tianjin, China. Particuology 7(6):432–437

McElroy MW, Carr RC, Ensor DS, Markowski GR (1982) Size distribution of fine particles from coal combustion. Science 215:13–19

Meng ZY, Jiang XM, Yan P, Lin WL, Zhang HD, Wang Y (2007) Characteristics and sources of PM2.5 and carbonaceous species during winter in Taiyuan, China. Atmos Environ 41:6901–6908

Saarikoski S, Timonen H, Saarnio K, Aurela M, Järvi L, Keronen P et al (2008) Sources of organic carbon in fine particulate matter in northern European urban air. Atmos Chem Phys 8:6281–6295

Saylor RD, Edgerton ES, Hartsell BE (2006) Linear regression techniques for use in the EC tracer method of secondary organic aerosol estimation. Atmos Environ 40(39):7546–7556

Schneidemesser E, Zhou JB, Stone EA, Schauer JJ, Qasrawi R, Abdeen Z et al (2010) Seasonal and spatial trends in the sources of fine particle organic carbon in Israel, Jordan, and Palestine. Atmos Environ 44: 3669–3678

Schwier AN, Sareen N, Mitroo D, Shapiro EL, McNeill VF (2010) Glyoxal-methylglyoxal cross-reactions in secondary organic aerosol formation. Environ Sci Technol 44(16):6174–6182

Sun H, Biedermann L, Bond TC (2007) Color of brown carbon: a model for ultraviolet and visible light absorption by organic carbon aerosol. Geophys Res Lett 34, L17813

Turpin BJ, Huntzicker JJ, Larson SM, Cass GR (1991) Los Angeles summer midday particulate carbon: primary and secondary aerosol. Environ Sci Technol 25(10):1788–1793

Wang G, Li J, Cheng C, Hu S, Xie M, Gao S et al (2011a) Observation of atmospheric aerosols at Mt. Hua and Mt. Tai in central and east

China during spring 2009 – Part 1: EC, OC and inorganic ions. Atmos Chem Phys 11:4221–4235

Wang Y, Xin J, Li Z, Wang S, Wang P, Hao WM, et al. (2011b). Seasonal variations in aerosol optical properties over China. J Geophys Res: Atmos 116:D18

Wang R, Tao S, Wang W, Liu J, Shen H et al (2012) Black carbon emissions in China from 1949 to 2050. Environ Sci Technol 46(14):7595–7603

Watson JG, Chow JC, Houck JE (2001) PM2.5 chemical source profiles for vehicle exhaust, vegetative burning, geological material, and coal burning in Northwestern Colorado during 1995. Chemosphere 43:1141–1151

Yan P, Xun N, Zhang YM (2012) Measurements of carbonaceous aerosol in rural area in Beijing. J Appl Meteorol Sci 23(3):285–293

Yang M, Howell S, Zhuang J, Huebert B (2009) Attribution of aerosol light absorption to black carbon, brown carbon, and dust in China–

interpretations of atmospheric measurements during EAST-AIRE. Atmos Chem Phys 9:2035–2050

Yu H, Wu C, Wu D, Yu J (2010) Size distributions of elemental carbon and its contribution to light extinction in urban and rural locations in the pearl river delta region, China. Atmos Chem Phys 10:5107–5119

Zhang XY, Wang YQ, Zhang XC, Guo W, Gong SL (2008) Carbonaceous aerosol composition over various regions of China during 2006. J Geophys Res 113, D14111

Zhang RJ, Tao J, Ho KF, Shen ZX, Wang GH, Cao JJ et al (2012) Characterization of atmospheric organic and elemental carbon of $PM_{2.5}$ in a typical semi-arid area of Northeastern China. Aerosol Air Qual Res 12:792–802

Zhou JM, Zhang RJ, Cao JJ, Chow JC, Watson JG (2012) Carbonaceous and ionic components of atmospheric fine particles in Beijing and their impact on atmospheric visibility. Aerosol Air Qual Res 12: 492–502